JACS
JOURNAL OF THE AMERICAN CHEMICAL SOCIETY
pubs.acs.org/JACS
Article

# Tunable Multisite Proton-Coupled Electron Transfer Mediators: Distinct Pathways for Substrate Reduction Versus Competing Hydrogen Evolution

John M. Ovian,[‡] Joseph Derosa,[‡] Mengdi Li, and Jonas C. Peters*

Cite This: J. Am. Chem. Soc. 2026, 148, 2609−2616
Read Online
ACCESS | Metrics & More | Article Recommendations | Supporting Information

**ABSTRACT:** Proton-coupled electron transfer (PCET) reagents have emerged as powerful tools for transferring net H atoms to organic substrates from relatively weak X−H bonds. One advantage of employing PCET reagents is the tunability of the X−H bond strength by independently varying their redox potential and/or p$K_a$ for selective substrate reductions; however, the rational development of modular catalytic PCET reagents based on these features remains underdeveloped. Here, we address important mechanistic questions relevant to a dimethylaniline-appended cobaltocene PCET mediator that our lab has previously introduced. Specifically, we examine where protonation occurs within the reactive Co(II, NH)$^+$ intermediate of a Brønsted-base modified cobaltocene mediator, whether substrate reduction and hydrogen evolution reaction (HER) proceed by a common or bifurcated mechanistic pathway, and how the redox, acid−base, and structural properties of PCET mediators can dictate their reactivity and selectivity. We show that substrate compatibility can be tuned and, via a model study with *N*-aryl imine substrates, provide data pointing to a multisite PCET (MS-PCET) pathway. Moreover, we rigorously characterize the site of protonation in the reactive reduced, protonated form of the mediator, and through kinetic analysis establish that the pathway for undesired competing HER is fundamentally different and involves Cp-ring protonation. Our findings point to a high degree of flexibility in the design of reductive PCET mediators.

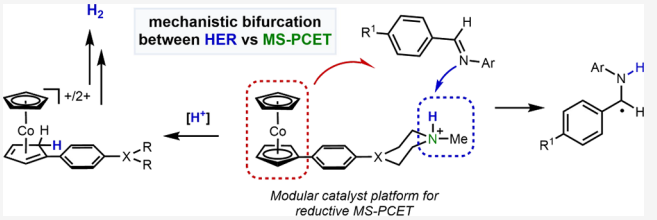


## INTRODUCTION

The ability to distinguish between unsaturated bonds (e.g., C = O, C = N, C = C) in organic substrate reductions is valuable in complex syntheses.[1] Proton-coupled electron transfer (PCET) has emerged as an appealing strategy for carrying out reductive organic transformations at lower driving force than stepwise proton and electron transfer.[2,3] Tuning the reduction potential and/or the p$K_a$ of the PCET reagent directly influences the driving force of net H atom transfer to a substrate; this modularity is highly appealing for the development of chemoselective PCET processes through reagent design.[4−7] Despite this, the development of tunable reductive PCET catalysts is underexplored.[8]

When designing new PCET mediators, it is important to consider the mechanism by which they operate. Two limiting pathways can be delineated for concerted reductive PCET: hydrogen-atom transfer (HAT) and multisite PCET (MS-PCET) (Figure 1A).[9] Whereas HAT involves the concerted transfer of a hydrogen atom from the donor to an acceptor in a single step, MS-PCET refers to processes where the proton and electron are transferred from different sites, either on the same or different molecules.[3,10] Such mechanistic distinctions can have implications for new reagent and reaction design, as has been reported by various laboratories.[8−13] Specifically, while reductive HAT reagents have proven highly useful,[14] they can suffer from kinetic and thermodynamic limitations if accessed electrocatalytically with a proton source. This is because protonation at the metal to furnish a metal hydride (M−H) is often accompanied by a second electron transfer that leads to a competitive hydrogen evolution reaction (HER):

$$(M - H) + e^- \rightarrow (M - H)^-;\ (M - H)^- + H^+ \rightarrow H_2 + M \quad (1)$$

In contrast, a MS-PCET strategy can afford selective access to intermediates containing weak X−H bonds (<50 kcal/mol) (e.g., using a phosphoric acid and iridium photocatalyst).[9,15] Our laboratory has described an electrocatalytic PCET (*e*PCET) mediator comprised of an *N*,*N*-dimethylaniline-appended cobaltocene (Figure 1B), with a homolytically weak N−H bond in its reduced protonated state (Co(II, NH)$^+$; BDFE$_{N-H}$ = 37 kcal/mol).[16] This state is kinetically stable to

Received: October 20, 2025
Revised: December 16, 2025
Accepted: December 18, 2025
Published: January 7, 2026







https://doi.org/10.1021/jacs.5c18522
J. Am. Chem. Soc. 2026, 148, 2609−2616

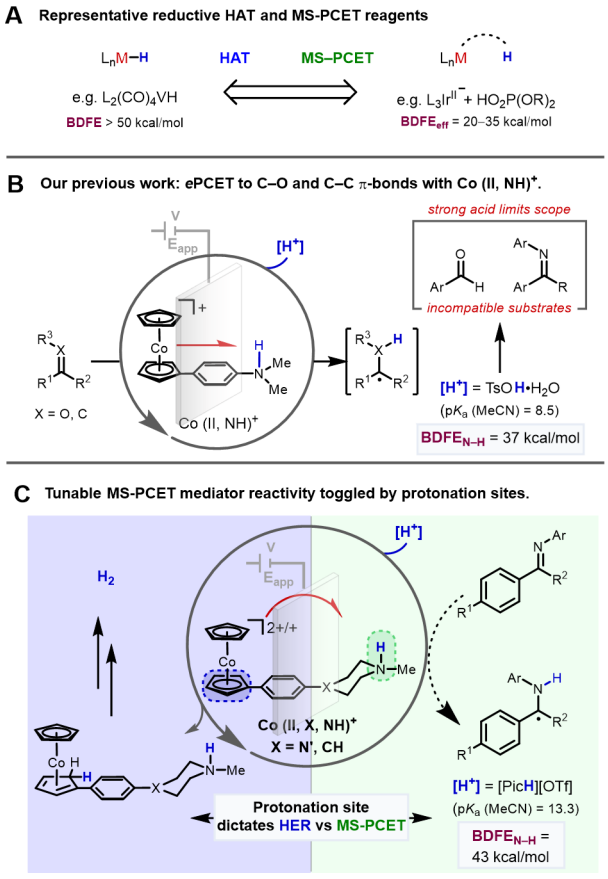


**Figure 1.** (A) Representative examples of reductive HAT[22] and MS-PCET reagents.[15] (B) Prior studies of an aniline-appended cobaltocene PCET mediator. (C) Design of amine-appended cobaltocene mediators featured in this study.

HER, enabling its use under controlled potential electrolysis at −1.30 V vs $Fc^{+/0}$ (all potentials herein referenced to $Fc^{+/0}$) to perform *e*PCET to aryl ketones,[17] activated alkenes,[18] and in tandem electrocatalysis for $N_2$ reduction[19] and hydride transfer reactions.[20]

Our prior reports have posited several ideas important to future PCET mediator designs that merit closer examination. Some of these are pertinent to the present study, as follows:

1) Is a MS-PCET the best descriptor for the pathway of substrate reduction between the reduced-protonated form of the mediator ($Co(II, NH)^+$) and substrate? To address this issue, it is paramount to establish where the proton resides in the reactive $Co(II, NH)^+$ state. It has been assumed to reside at the N atom of the N,N-dimethylaniline group, but this has yet to be firmly shown. Even if such an assignment is correct, whether the proton migrates from the appended base to the Cp-ring prior to the net H atom transfer step remains an open question and should also be addressed.
2) Relatedly, if an MS-PCET pathway is relevant to substrate reduction, is such a pathway also relevant to competing HER, or is a distinct mechanism operative, thereby bifurcating selectivity between substrate reduction and HER? We have previously speculated that $Co(II, NH)^+$ shows attenuated reactivity toward HER because of the cost of bringing two cations together in a bimolecular step relative to a more favorable reaction with an uncharged substrate present at higher concentration than $Co(II, NH)^+$. This argument follows from a conservation of mechanism for both substrate reduction and HER and needs to be tested. An appealing alternative would be that HER follows a more conventional Cp-ring protonation pathway, ideally showing a distinct kinetic signature.
3) Mechanistic understanding will guide the design of mediators, with important parameters including tunable bond-dissociation free energy (BDFE) values, underlying redox potentials, $pK_a$ values, and correlated patterns of reactivity. Relatedly, for cobaltocene mediators of the present type one should consider what types of spacers and special separation between the metallocene redox subunit and the proton relay are compatible with MS-PCET, and how the $pK_a$ of the appended base (or, conversely, the cobaltocene subunit) impacts substrate versus HER selectivity and substrate scope.

The present experimental study begins to address each of these important issues. Here we focus on a cobaltocene bearing an isolated tertiary amine as a useful experimental probe. Specifically, we envisioned that *N*′-phenyl-*N*-methylpiperazine-appended cobaltocene mediator ($Co(II, N', N)$; Figure 1C) could be protonated by a weaker acid at the distal nitrogen ($Co(II, N', NH)$). Moving to a more-basic amine protonation site results in substantial strengthening of the N−H bond ($BDFE_{N-H}$ = 43 kcal/mol) relative to the parent mediator, well-matched for reactivity with imine substrates ($BDFE_{N-H}$ (calc) = 50 kcal/mol), making this an effective model system for PCET reactivity.[21]

## RESULTS AND DISCUSSION

Using 4-bromo-*N*′-phenyl-*N*-methylpiperazine as a precursor, the desired $Co(III, N', N)^+$ compound (Figure 2) was

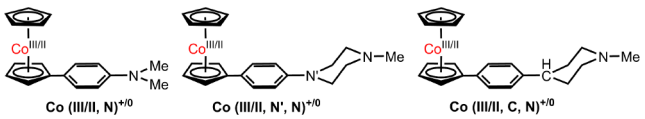


**Figure 2.** Structures and associated naming system of base-appended cobaltocenes discussed in this study.

prepared in analogy to previously reported $Co(III, N)^+$.[16] We measured the $pK_a$ of $Co(III, N', NH)^{2+}$ in MeCN to be 15.6.[23] Cyclic voltammetry (CV) of $Co(III, N', N)^+$ at 100 mV/s with 100 mM $TBAPF_6$ electrolyte in MeCN shows a reversible Co (III/II) reduction at −1.35 V and an irreversible oxidation feature at 0.58 V. We assign the oxidative features to *N*-centered oxidation, consistent with reported amine oxidations.[24] The Co(III/II) redox couple at −1.35 V is unperturbed upon addition of 20 mM picolinium triflate ([PicH][OTf]; $pK_a$ (MeCN) = 13.3), whereas the oxidative feature at 0.58 V vanishes, consistent with protonation to form $Co(III, N', NH)^{2+}$; these data provide a $BDFE_{N-H}$ of 43 kcal/mol (Figure 3A).

Having performed our thermochemical measurements in MeCN, we evaluated the reductive protonation of imines in 1,2-dimethoxyethane (DME), in which the $BDFE_{N-H}$ is anticipated to be similar.[25] Addition of 10 mM imine substrate causes the wave at −1.35 V to become irreversible, rising in current, indicative of electrocatalysis (Figure 3B). We


https://doi.org/10.1021/jacs.5c18522
J. Am. Chem. Soc. 2026, 148, 2609−2616

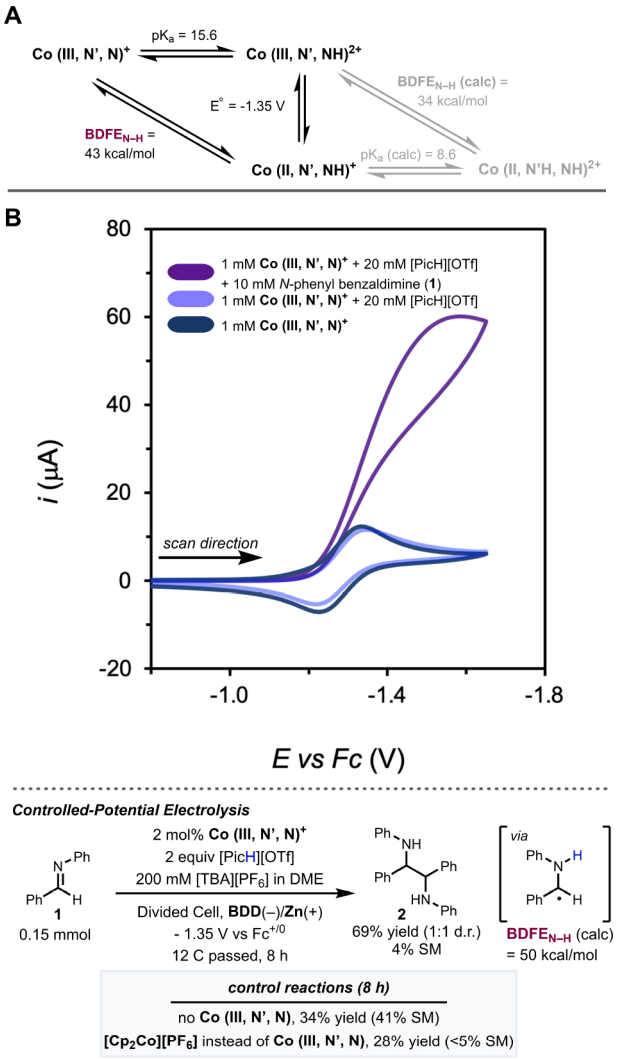


**Figure 3.** (A) Thermochemical considerations for accessing Co (II, N', NH)$^+$. (B) CVs corresponding to color coded inset legend (top) and CPE using Co(III, N', N)$^+$ with *N*-phenyl benzaldimine substrate (1) and [PicH][OTf] at −1.35 V vs $Fc^{+/0}$ (bottom). CV conditions: scan rate = 100 mV/s, 100 mM [TBA][$PF_6$] in DME using a boron-doped diamond (BDD) disk working electrode, glassy carbon (GC) disk counter electrode, and Ag/AgOTf reference. CPE conditions: divided cell using a BDD plate working electrode, Zn foil counter electrode, and Ag/AgOTf reference.

conducted controlled potential electrolysis (CPE) at −1.35 V with 2 mol % Co(III, N', N)$^+$, 0.15 mmol of *N*-phenyl benzaldimine, and 0.3 mmol of [PicH][OTf], with 200 mM [TBA][$PF_6$] as electrolyte in DME. After the passage of 12 C, imino-pinacol product **2** was confirmed in 69% yield (1:1 d.r.), with 4% **1** remaining. While the reaction proceeds without the addition of Co(III, N', N)$^+$ in 34% yield, only 41% of the starting material remains; using 2 mol % [$Cp_2Co$][$PF_6$] instead of Co(III, N', N) gives similarly poor performance (28% yield of **2** with <5% starting material remaining).

To probe the chemoselectivity of the *e*PCET process using a weaker acid, we wondered whether these conditions would be amenable to an in situ protocol using aniline and benzaldehyde as starting materials. With TsOH·$H_2O$, which is required to protonate our first-generation mediator, Co(III, N)$^+$, benzaldehyde substrates suffered from deleterious electrode-mediated decomposition. Given an estimated $BDFE_{O-H}$ of 37 kcal/mol for the benzaldehyde ketyl radical,[26] we intuited that Co (II, N', NH)$^+$ might be selective for net H atom delivery only to the condensed imine product ($BDFE_{N-H}$ of 50 kcal/mol for *α*-amino radical intermediate; Figure 4A).

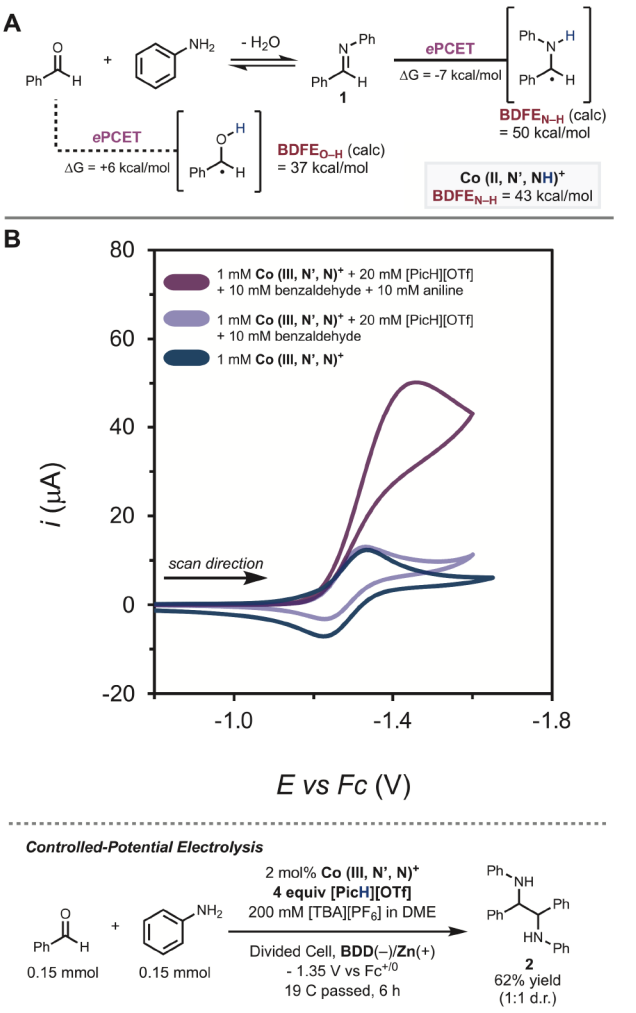


**Figure 4.** (A) Thermochemical considerations for PCET to either benzaldehyde or 1 using Co(II, N', NH)$^+$. (B) CVs corresponding to color coded inset legend (top) and CPE using *in situ* condensation protocol (bottom). CV conditions: Scan rate = 100 mV/s, 100 mM [TBA][$PF_6$] in DME using a BDD disk working electrode, GC disk counter electrode, and Ag/AgOTf reference. CPE conditions: Divided cell using a BDD plate working electrode, Zn foil counter electrode, and Ag/AgOTf reference.

CV experiments in the presence of 10 mM benzaldehyde and 20 mM [PicH][OTf] showed that the Co(III/II) couple remains reversible (Figure 4B). Upon addition of 10 mM aniline to the cell with stirring for 30 s, however, the Co(III/II) couple becomes irreversible, consistent with *e*PCET to in situ-generated **1**. Under slightly modified CPE conditions, with 4 equiv of [PicH][OTf] and a 1:1 mixture of benzaldehyde to aniline, the desired imino-pinacol coupling product **2** was generated in 62% yield (1:1 d.r.).

To investigate the nature of the PCET step, further CV studies were carried out to obtain kinetic data pertinent to electrocatalysis.[27,28] With benzaldimine **1** as the substrate the rate was found to be first order in **1** (Figure 5A), zeroth order in [PicH][OTf] (Figure 5B), and first order in cobalt (see


https://doi.org/10.1021/jacs.5c18522
J. Am. Chem. Soc. 2026, 148, 2609−2616

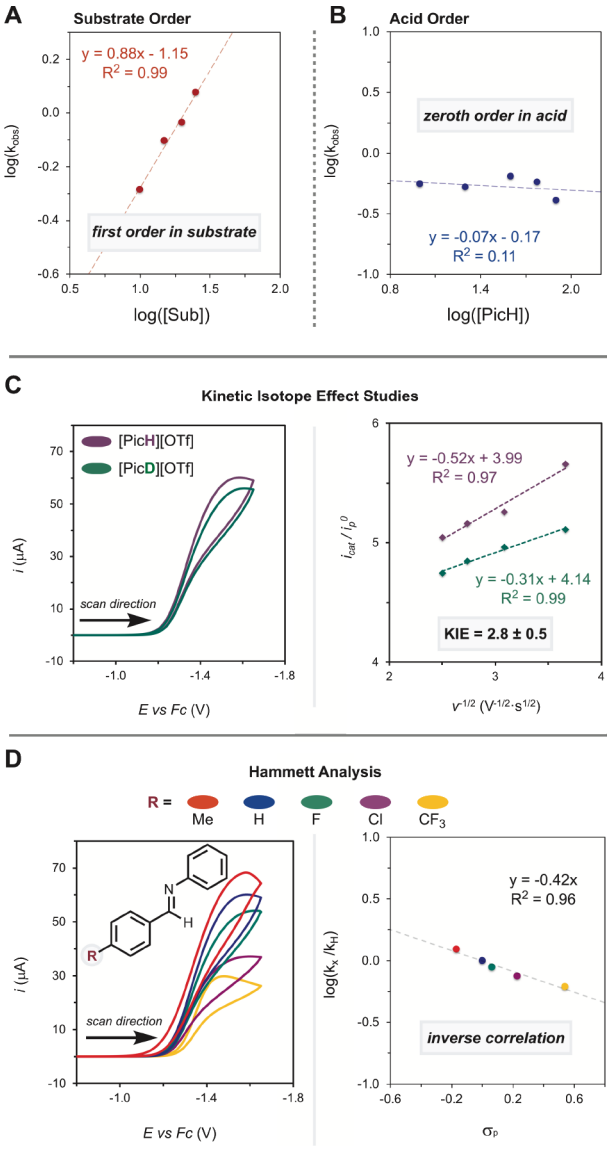


**Figure 5.** (A) Plot of $\log(k_{obs})$ with respect to log([1]). (B) Plot of $\log(k_{obs})$ with respect to $\log([PicH]^+)$. (C) Comparison of CVs taken at 100 mV/s with [PicH][OTf] (purple) and [PicD][OTf] (green). (D) CVs of *para*-substituted *N*-aryl benzaldimines and Hammett analysis; CV conditions: Scan rate = 100 mV/s, 1 mM Co(III, N', N)$^+$, 10 mM imine, 20 mM [PicH][OTf], 100 mM [TBA][$PF_6$] in DME using a BDD disk working electrode.

Supporting Information, Figure S39). Comparing [PicH]-[OTf] versus [PicD][OTf] afforded a kinetic isotope effect (KIE) of 2.8 ± 0.5 (Figure 5C).[16] Comparing the relative rates of *para*-substituted *N*-phenyl benzaldimines (R = Me, F, Cl, $CF_3$; Figure 5D) via a Hammett plot analysis reveals a linear correlation with a small negative slope, indicative of a buildup of slight positive charge in the transition state.[29−31] Such a model would be consistent with H-bonding between the mediator and the imine in an association complex equilibrium of the MS-PCET process. These results are in accord with our previous study using substituted acetophenones and the parent mediator Co(III, N)$^+$ in the presence of TsOH•$H_2O$.[16] The trend also holds with *para*-substitution on the aniline component (see Supporting Information, Figure S41). Collectively, the data are consistent with a rate-limiting PCET step to form an alpha-amino radical, followed by imino-pinacol homocoupling.

Based on anticipated differences in basicity, we have inferred that only distal N-protonation is accessible for Co(II, N', N) using [PicH][OTf]. However, in our prior reports using Co(II, N) as an *e*PCET mediator we have inferred, but not explicitly characterized, the structure of the protonated Co(II)$^+$ form. We were therefore interested in firmly establishing the location of the proton, i.e. whether it rests on the aniline nitrogen as anticipated, or possibly on a ring of the cobaltocene subunit instead (Figure 6A).[32] Knowledge of this is critical to mapping the competing pathway for HER, as discussed next.

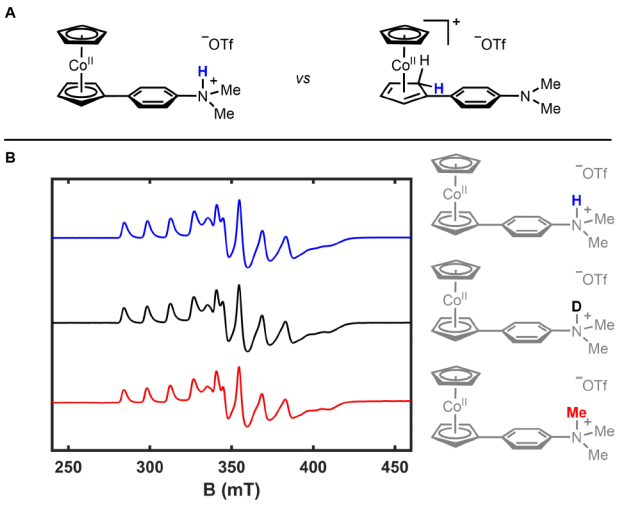


**Figure 6.** CW X-band EPR spectra of protonated (blue), deuterated (black), and methylated (red) Co(II, N).

To address the protonation site, we synthesized a trimethylanilinium analog, Co(II, NMe)$^+$, of the putative N-protonated form, and compared its spectral and electrochemical features with those of the in situ-formed, Co(II, NH)$^+$. Protonation at the cobaltocene core (either at Cp or Co) is expected to give rise to significant differences in the continuous wave-electron paramagnetic resonance (CW-EPR) spectra of Co(H/D) (II, N) $^+$ and Co(II, NMe)$^+$.

X-band CW-EPR spectra at 10 K in THF of the proton and deuteron isotopologues (formed in situ by reaction with 2-methoxypyridinium triflate, [$^{2\text{-OMe}}$PyrH or D][OTf]) are indistinguishable from one another and from the methylated analog (Figure 6B, Figure S20 for simulation). Further, the protonated and methylated complexes show very similar UV−vis absorption profiles, and analogous Co(III/II) redox couples, respectively (see Figures S1 and S2). Taken together, these data verify that the protonation site is indeed the aniline nitrogen, as expected; the unpaired spin is localized on the cobaltocene subunit. This conclusion supports the idea that the base-appended cobaltocene platform acts as a unimolecular MS-PCET mediator rather than as an H atom shuttle.

Next, we addressed whether isomerization from the anilinium form to a Cp-ring-protonated species might be necessary for productive PCET-to-substrate reactivity. To probe this possibility, we focused on the mechanism for competitive HER. While previous studies have suggested that HER by cobaltocenes primarily occurs through Cp or Co protonation,[31,33] we have wondered whether HER mediated by Co(II, NH)$^+$ might occur through a bimolecular mechanism


https://doi.org/10.1021/jacs.5c18522
J. Am. Chem. Soc. 2026, 148, 2609−2616

with MS-PCET character given its weak $BDFE_{N-H}$ of 37 kcal/mol.[16]

To address this issue experimentally, we designed a base-appended cobaltocene mediator bearing an *N*-methyl-4-phenylpiperidine moiety, Co(II, C, N), to deconvolute effects of N-protonation on the cobaltocene fragment (Figure 7A).

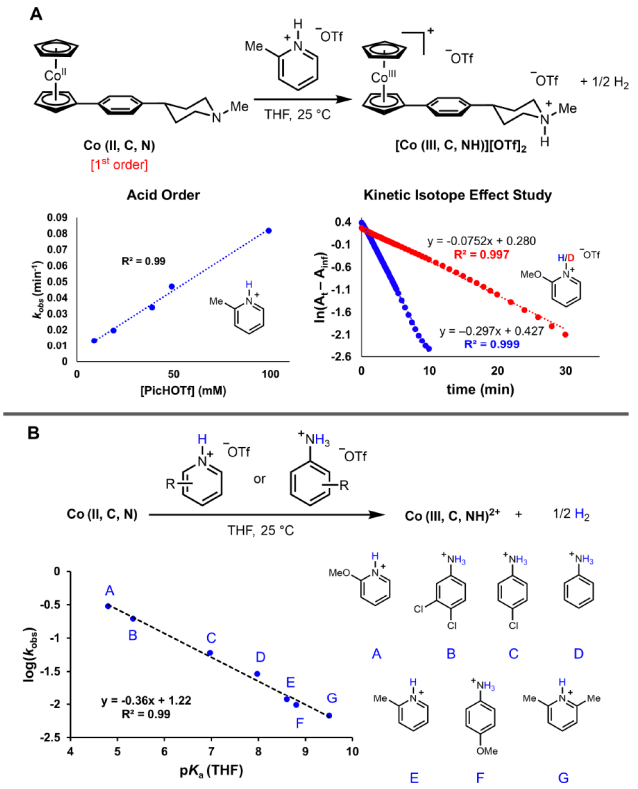


**Figure 7.** (A) Kinetic analysis of HER and kinetic isotope effect study. (B) Comparison of rate of hydrogen evolution by different Brønsted acids.

Addition of [PicH][OTf] ($pK_a$ (THF) = 8.6) to Co(II, C, N) resulted in an 8 nm red shift in the spectrum, assigned to Co(II, C, NH)$^+$ (Figure S45). Following the decay of the Co(II) feature at 544 nm, we observed a first-order decay to its oxidized form, and formation of $H_2$ confirmed by GC analysis of the headspace (Figure 7A). Tight isosbestic points observed in the UV−vis time course indicate that there is no buildup of another intermediate.

Most strikingly, the rate of HER with [PicH][OTf] is first order in acid (Figure 7A), implying a mechanism distinct from substrate (imine/ketone) reductions, which show zero-order dependence on acid concentration. To rule out a mechanism that proceeds through rate-limiting reduction of the acid by Co(II), we measured the observed rates ($k_{obs}$) of HER for various electronically and sterically differentiated anilinium and pyridinium Brønsted acids (Figure 7B). The observed rates correlate well with the reported $pK_a$ values in THF[34] ($\alpha$ = 0.36) of the acids and not with their expected 1-electron reduction potentials (where the anilinium acids should behave differently from the pyridinium acids). Furthermore, we measured a primary KIE of 3.9 on deuteration of [$^{2\text{-OMe}}$PyrH][OTf] (Figure 7A). While the absolute activity of the acids in THF may be complicated by homoconjugation and/or sterics, it is clear that the observed rate of HER correlates well with independently measured $pK_a$ values.[35] These data, taken together, are consistent with a rate-limiting proton transfer step. Analysis of the oxidized Co(III, C, N)$^+$ reaction product revealed no incorporation of deuterium into any position, consistent with Co-centered, *ipso* or stereospecific protonation/hydrogen-evolution mechanisms.

On the basis of these and other studies,[33,36−39] we propose the HER mechanism depicted in Figure 8A. Rate-limiting

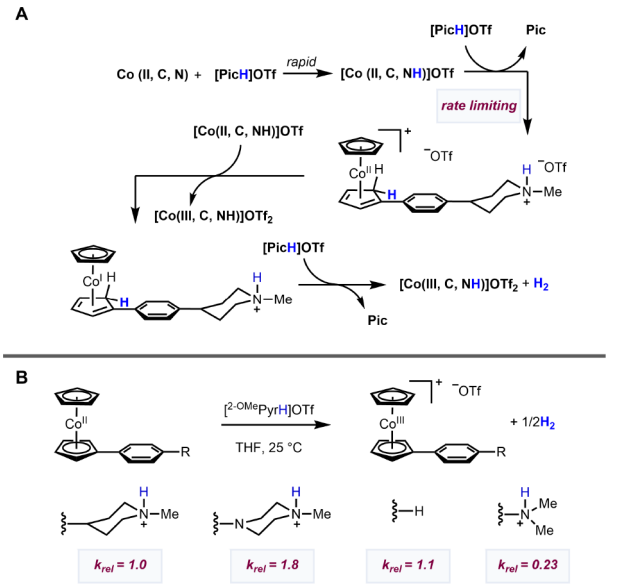


**Figure 8.** (A) Proposed mechanism for hydrogen evolution reaction by base-appended cobaltocenes. (B) Structure−activity relationship study of base-appended cobaltocenes on rate of HER.

protonation of the Cp ring of Co(II, C, NH)$^+$ forms an electron deficient Co(II) dienyl cation. The Co(II/I) redox couple of this species is estimated to be shifted about 1 V positive[31,40] of the Co(III/II) couple, enabling rapid reduction by [Co(II, C, NH)]OTf to a Co(I) species possessing a hydridic Cp-H[32,33,36,40] capable of protonation by the acid to generate $H_2$ and return the oxidized Co (III, C, NH)$^+$. This HER mechanism is satisfying in that it parallels the HER mechanism proposed for cobaltocene itself and is distinct from the MS-PCET pathway operative for substrate reductions.[32,33]

An important issue for mediator design arising from the above discussion concerns the comparative basicity of the cobaltocene subunit as a function of the mediator structure; this issue should correlate with competing HER. We hence compared the rates of HER between different mediators to gauge the comparative basicity of the cobaltocene core (Figure 8B).

Using [$^{2\text{-OMe}}$PyrH][OTf], a sufficiently strong acid to protonate Co(II, N) and Co(II, N', N) at N, we find that the rate of HER by Co(II, C, N) is ∼ 4 times faster than Co(II, N). This observation suggests that *N*-protonation of Co(II, N) inhibits HER by inductively diminishing the basicity of the cobaltocene subunit (i.e., it serves as an electron-withdrawing group). To account for confounding charge effects, we also synthesized and measured the rate of HER by phenyl-substituted cobaltocene. The rate is very similar to Co(II, C, N), indicating charge repulsion between the cationic ammonium and the pyridinium acid has a minimal inhibitory effect. Finally, comparing Co(II, C, N) to Co(II, N', N), the latter is oxidized significantly faster by [$^{2\text{-OMe}}$PyrH][OTf]. We


https://doi.org/10.1021/jacs.5c18522
J. Am. Chem. Soc. 2026, 148, 2609−2616

infer that protonation of the distal N in Co(II, N', N) lowers the p$K_a$ of N' to such a degree that the cobaltocene fragment is competitively basic. At the same time, the electron-donating nature of N' likely increases the basicity of the Cp ring relative to Co(II, C, N). Importantly, these observations collectively establish that the basicity of the cobaltocene subunit of the mediator is the primary feature dictating competing HER.

Given that the active parent mediator state, Co(II, NH)$^+$, appears to have minimal spin-density delocalized onto the anilinium, we wondered whether the site-isolated Co(II, C, NH)$^+$ could still act as a multisite PCET reagent, or if rearrangement to the aniline-protonated isomer of Co (II, N', NH)$^+$, i.e. Co(II, N'H, N)$^+$, is instead necessary for PCET reactivity. Under conditions with no observable rate of HER (eq 2), addition of imine to Co(II, C, NH)$^+$ yielded rapid

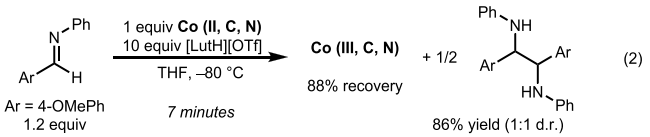


formation of the diamine product (86% yield, 1:1 dr) and Co(III, C, N)$^+$ (88% recovery). The rapid reaction of the Co(II, C, NH)$^+$ with the imine supports our proposed mechanism of productive PCET reactivity occurring through the distal N-protonated form, and not via isomerization to a ring- or aniline-protonated form. Hence, we infer that distinct catalytic cycles are at play for HER versus substrate reduction, as generalized in Figure 9.

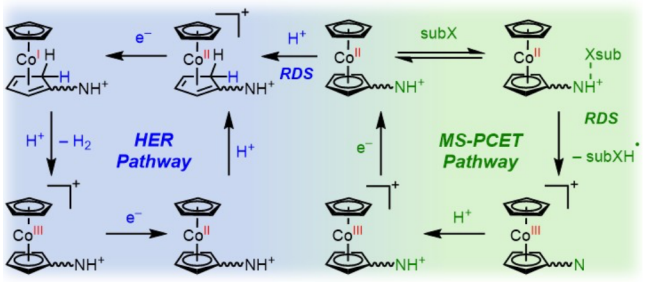


**Figure 9.** Bifurcating pathways for HER versus MS-PCET substrate reduction by Brønsted-base modified cobaltocene mediators.

## CONCLUSIONS

To close, in this study we have elucidated the site of protonation in the reactive Co(II, NH)$^+$ intermediate, determined that substrate reduction and hydrogen evolution proceed by bifurcated mechanistic pathways, and examined how the redox, acid–base, and structural properties of PCET mediators dictate their reactivity and selectivity. To address these issues, we prepared new mediators with modified p$K_a$'s, dependent on protonation site and correlated p$K_a$ strength of the acid employed. This approach enabled imino-pinacol coupling reactivity, which was previously inaccessible owing to a much strong acid (tosic acid) being necessary for the parent mediator. The design of these new mediators has enabled definitive experiments critical to understanding their mechanistic nuances. Most notably, we have verified the *N*-atom of the Brønsted-base appendage to be the site of protonation in the reactive Co(II) state, and our data are consistent with a unimolecular MS-PCET mechanism, independent of acid concentration, for substrate reduction. However, mechanistic bifurcation between productive PCET and undesired HER is at play, with HER following an acid-dependent first-order rate that mostly likely occurs via protonation of a Cp ring on the cobaltocene subunit (see Figure 9). These findings point toward a highly flexible design of base-appended cobaltocenes for targeting selective PCET reactivity in future studies.

## ASSOCIATED CONTENT

### Supporting Information

The Supporting Information is available free of charge at https://pubs.acs.org/doi/10.1021/jacs.5c18522.

DFT coordinates (TXT)

Experimental procedures and methods, including synthesis and characterization of compounds, electrochemical data and procedures, thermochemical considerations, details of DFT calculations, and Cartesian coordinates (PDF)

### Accession Codes

Deposition Numbers 2496757–2496760 contain the supplementary crystallographic data for this paper. These data can be obtained free of charge via the joint Cambridge Crystallographic Data Centre (CCDC) and Fachinformationszentrum Karlsruhe Access Structures service.

## AUTHOR INFORMATION


### Corresponding Author

**Jonas C. Peters** – *Division of Chemistry and Chemical Engineering, California Institute of Technology (Caltech), Pasadena, California 91125, United States;* orcid.org/0000-0002-6610-4414; Email: jpeters@caltech.edu

### Authors

**John M. Ovian** – *Division of Chemistry and Chemical Engineering, California Institute of Technology (Caltech), Pasadena, California 91125, United States;* orcid.org/0000-0001-5362-5010

**Joseph Derosa** – *Division of Chemistry and Chemical Engineering, California Institute of Technology (Caltech), Pasadena, California 91125, United States;* orcid.org/0000-0001-8672-4875

**Mengdi Li** – *Division of Chemistry and Chemical Engineering, California Institute of Technology (Caltech), Pasadena, California 91125, United States;* orcid.org/0000-0002-6198-8396

Complete contact information is available at: https://pubs.acs.org/10.1021/jacs.5c18522

### Author Contributions

‡J.M.O. and J.D. contributed equally.


### Notes

The authors declare no competing financial interest.

## ACKNOWLEDGMENTS

We thank the Dow Next Generation Educator Funds and Instrumentation Grants for their support of the NMR facility at Caltech. The authors are grateful to the Department of Energy Basic Energy Sciences for support via Grant No. DE-SC0019136 and also to the American Chemical Society

Petroleum Research Fund (PRF# 61951-ND3). J.D. thanks the Arnold and Mabel Beckman Foundation for a postdoctoral fellowship, and J.C.P. is grateful to the Resnick Sustainability Institute for enabling facilities. J.M.O. thanks the National Institute of General Medical Sciences of the National Institutes of Health (NIH) for a postdoctoral fellowship (F32GM151784). The content is solely the responsibility of the authors and does not necessarily represent the official views of the NIH. We thank Dr. Paul Oyala (Caltech) for assistance in collecting EPR spectra.

## REFERENCES

(1) Shenvi, R. A.; O'Malley, D. P.; Baran, P. S. Chemoselectivity: The Mother of Invention in Total Synthesis. *Acc. Chem. Res.* **2009**, *42*, 530−541.
(2) Miller, D. C.; Tarantino, K. T.; Knowles, R. R. Proton-Coupled Electron Transfer in Organic Synthesis: Fundamentals, Applications and Opportunities. *Top. Curr. Chem.* **2016**, *374* (3), 30.
(3) Murray, P. R. D.; Cox, J. H.; Chiappini, N. D.; Roos, C. B.; McLoughlin, E. A.; Hejna, B. G.; Nguyen, S. T.; Ripberger, H. H.; Ganley, J. M.; Tsui, E.; Shin, N. Y.; Koronkiewicz, B.; Qiu, G.; Knowles, R. R. Photochemical and Electrochemical Applications of Proton-Coupled Electron Transfer in Organic Synthesis. *Chem. Rev.* **2022**, *122*, 2017−2291.
(4) Mayer, J. M. Proton-Coupled Electron Transfer: A Reaction Chemist's View. *Annu. Rev. Phys. Chem.* **2004**, *55*, 363−390.
(5) Agarwal, R. G.; Coste, S. C.; Groff, B. D.; Heuer, A. M.; Noh, H.; Parada, G. A.; Wise, C. F.; Nichols, E. M.; Warren, J. J.; Mayer, J. M. Free Energies of Proton-Coupled Electron Transfer and Their Applications. *Chem. Rev.* **2022**, *122*, 1−49.
(6) Komar, S. S.; Mayer, J. M. $SmI_2(H_2O)_n$ Reduction of Electron Rich Enamines by Proton-Coupled Electron Transfer. *J. Am. Chem. Soc.* **2017**, *139*, 10687−10692.
(7) Tyburski, R.; Hammarström, L. Strategies for Switching the Mechanism of Proton-Coupled Electron Transfer Reactions Illustrated by Mechanistic Zone Diagrams. *Chem. Sci.* **2021**, *13*, 290−301.
(8) Qiu, G.; Knowles, R. R. Rate−Driving Force Relationships in the Multisite Proton-Coupled Electron Transfer Activation of Ketones. *J. Am. Chem. Soc.* **2019**, *141*, 2721−2730. Modularity of photocatalytic multisite PCET systems have been studied by Knowles and coworkers in the context of ketyl radical generation:
(9) Darcy, J. W.; Koronkiewicz, B.; Parada, G. A.; Mayer, J. M. A Continuum of Proton-Coupled Electron Transfer Reactivity. *Acc. Chem. Res.* **2018**, *51*, 2391−2399.
(10) Mayer, J. M. Understanding Hydrogen Atom Transfer: From Bond Strengths to Marcus Theory. *Acc. Chem. Res.* **2011**, *44*, 36−46.
(11) Jabalera-Ortiz, P. J.; Perona, C.; Moreno-Albarracín, M.; Carmona, F. J.; Jiménez, J.-R.; Navarro, J. A. R.; Garrido-Barros, P. Reductive Photocatalytic Proton-Coupled Electron Transfer by a Zirconium-Based Molecular Platform. *Angew. Chem., Int. Ed.* **2024**, *63*, No. e202411867.
(12) Nocera, D. G. Proton-Coupled Electron Transfer: The Engine of Energy Conversion and Storage. *J. Am. Chem. Soc.* **2022**, *144*, 1069−1081.
(13) Ren, Y.; Yu, C.; Tan, X.; Huang, H.; Wei, Q.; Qiu, J. Strategies to Suppress Hydrogen Evolution for Highly Selective Electrocatalytic Nitrogen Reduction: Challenges and Perspectives. *Energy Environ. Sci.* **2021**, *14*, 1176−1193.
(14) Green, S. A.; Crossley, S. W. M.; Matos, J. L. M.; Vásquez-Céspedes, S.; Shevick, S. L.; Shenvi, R. A. The High Chemofidelity of Metal-Catalyzed Hydrogen Atom Transfer. *Acc. Chem. Res.* **2018**, *51*, 2628−2640.
(15) Yayla, H. G.; Knowles, R. R. Proton-Coupled Electron Transfer in Organic Synthesis: Novel Homolytic Bond Activations and Catalytic Asymmetric Reactions with Free Radicals. *Synlett* **2014**, *25*, 2819−2826.
(16) Chalkley, M. J.; Garrido-Barros, P.; Peters, J. C. A Molecular Mediator for Reductive Concerted Proton-Electron Transfer via Electrocatalysis. *Science* **2020**, *369*, 850−854.
(17) Derosa, J.; Garrido-Barros, P.; Peters, J. C. *Inorg. Chem.* **2022**, *61*, 6672−6678.
(18) Derosa, J.; Garrido-Barros, P.; Peters, J. C. Electrocatalytic Reduction of C−C $\pi$-Bonds via a Cobaltocene-Derived Concerted Proton-Electron Transfer Mediator: Fumarate Hydrogenation as a Model Study. *J. Am. Chem. Soc.* **2021**, *143*, 9303−9307.
(19) Garrido-Barros, P.; Derosa, J.; Chalkley, M. J.; Peters, J. C. Tandem Electrocatalytic $N_2$ Fixation via Proton-Coupled Electron Transfer. *Nature* **2022**, *609*, 71−76.
(20) Derosa, J.; Garrido-Barros, P.; Li, M.; Peters, J. C. Use of a PCET Mediator Enabled a Ni-HER Electrocatalyst to Act as a Hydride Delivery Agent. *J. Am. Chem. Soc.* **2022**, *144*, 20118−20125.
(21) Cui, W.; Xu, X.; Zhang, C.; Wang, D.; Yang, Y.; Wang, Q.; Wang, J. Manganese-Promoted Electrochemical Imino-Pinacol Coupling to Access Vicinal Diamines. *J. Org. Chem.* **2025**, *90*, 3659−3664.
(22) Choi, J.; Pulling, M. E.; Smith, D. M.; Norton, J. R. Unusually Weak Metal-Hydrogen Bonds in $HV(CO)_4$(P-P) and Their Effectiveness as $H^\bullet$ Donors. *J. Am. Chem. Soc.* **2008**, *130*, 4250−4252.
(23) Kütt, A.; Tshepelevitsh, S.; Saame, J.; Lõkov, M.; Kaljurand, I.; Selberg, S.; Leito, I. Strengths of Acids in Acetonitrile. *Eur. J. Org. Chem.* **2021**, *2021*, 1407−1419.
(24) Smith, J. R. L.; Masheder, D. Amine Oxidation. Part IX. The Electrochemical Oxidation of Some Tertiary Amines: The Effect of Structure on Reactivity. *J. Chem. Soc., Perkin Trans. 2* **1976**, 47−51.
(25) Warren, J. J.; Tronic, T. A.; Mayer, J. M. Thermochemistry of proton-coupled electron transfer reagents and its implications. *Chem. Rev.* **2010**, *110*, 6961−7001.
(26) While our computationally obtained $BDFE_{X-H}$ values are internally consistent for this study, other values may be derived using different computational models, for example that of the benzaldehyde O−H ketyl radical species. Due to the uncertainty in the estimation of the free energy of $H^\bullet$, we address these discrepancies by attributing an error of ± 4 kcal/mol to all of our computationally derived $BDFE_{X-H}$ values.
(27) Costentin, C.; Savéant, J.-M. Multielectron, multistep molecular catalysis of electrochemical reactions: benchmarking of homogeneous catalysts. *ChemElectroChem.* **2014**, *1*, 1226−1236.
(28) Lee, K. J.; Elgrishi, N.; Kandemir, B.; Dempsey, J. L. Electrochemical and spectroscopic methods for evaluating molecular electrocatalysts. *Nat. Rev. Chem.* **2017**, *1*, No. 0039.
(29) Tyburski, R.; Liu, T.; Glover, S. D.; Hammarström, L. Proton-Coupled Electron Transfer Guidelines, Fair and Square. *J. Am. Chem. Soc.* **2021**, *143*, 560−576.
(30) Goetz, M. K.; Anderson, J. S. Experimental Evidence for pKa-Driven Asynchronicity in C−H Activation by a Terminal Co(III)-Oxo Complex. *J. Am. Chem. Soc.* **2019**, *141*, 4051−4062.
(31) The red trace in Figure 5D shows onset current slightly anodic of the other traces, which possibly arises from kinetically competitive PT-ET for this electron-rich imine substrate, or a modest background current from direct reduction by the electrode.
(32) Chalkley, M. J.; Del Castillo, T. J.; Matson, B.; Peters, J. C. Fe-Mediated Nitrogen Fixation with a Metallocene Mediator: Exploring $pK_a$ Effects and Demonstrating Electrocatalysis. *J. Am. Chem. Soc.* **2018**, *140*, 6122−6129.
(33) Koelle, U.; Infelta, P. P.; Graetzel, M. Kinetics and mechanism of the reduction of hydrogen by cobaltocene. *Inorg. Chem.* **1988**, *27*, 879−883.
(34) Garrido, G.; Rosés, M.; Ràfols, C.; Bosch, E. Acidity of Several Anilinium Derivatives in Pure Tetrahydrofuran. *J. Solution Chem.* **2008**, *37*, 689−700.
(35) Conway, B. E.; Wilkinson, D. P. Brønsted relationships for heterogeneous proton transfer at electrode interfaces. *J. Chem. Soc., Faraday Trans. 1* **1988**, *84*, 3389−3400. For a Brønsted study on heterogeneous HER in an organic solvent where a similar value was observed, see:


https://doi.org/10.1021/jacs.5c18522
J. Am. Chem. Soc. 2026, 148, 2609−2616

(36) Chalkley, M. J.; Oyala, P. H.; Peters, J. C. Cp* Noninnocence Leads to a Remarkably Weak C−H Bond via Metallocene Protonation. *J. Am. Chem. Soc.* **2019**, *141*, 4721−4729.
(37) Pitman, C. L.; Finster, O. N. L.; Miller, A. J. M. Cyclopentadiene-Mediated Hydride Transfer from Rhodium Complexes. *Chem. Commun.* **2016**, *52*, 9105−9108.
(38) Quintana, L. M. A.; Johnson, S. I.; Corona, S. L.; Villatoro, W.; Goddard, W. A.; Takase, M. K.; VanderVelde, D. G.; Winkler, J. R.; Gray, H. B.; Blakemore, J. D. Proton−hydride Tautomerism in Hydrogen Evolution Catalysis. *Proc. Natl. Acad. Sci. U. S. A.* **2016**, *113*, 6409−6414.
(39) Turner, G. K.; Kläui, W.; Scotti, M.; Werner, H. Studies on the Reactivity of Metal-$\pi$ Complexes XX. Evidence for the Stereospecific Ring Protonation of Nickelocene. *J. Organomet. Chem.* **1975**, *102*, C9−C11−C9−C11.
(40) Marron, D. P.; Galvin, C. M.; Dressel, J. M.; Waymouth, R. M. Cobaltocene-Mediated Catalytic Hydride Transfer: Strategies for Electrocatalytic Hydrogenation. *J. Am. Chem. Soc.* **2024**, *146*, 17075−17083.





https://doi.org/10.1021/jacs.5c18522
J. Am. Chem. Soc. 2026, 148, 2609−2616